NJC

ROYAL SOCIETY OF CHEMISTRY

PAPER

View Article Online
View Journal | View Issue

Cite this: *New J. Chem.*, 2020, 44, 2587

Evaluation of the supramolecular interaction of Congo red with cucurbiturils using mass spectrometry and spectroscopic methods†

Ana L. Costa, [a] Ana C. Gomes, [a] André D. Lopes, [b] José P. Da Silva, [b] Martyn Pillinger, *[a] Isabel S. Gonçalves [a] and J. Sérgio Seixas de Melo *[c]

The ability of cucurbit[*n*]urils (CB[*n*]) to decolourise aqueous solutions of the azo dye Congo red (CR) was described more than a century ago alongside the first synthesis of CB[*n*]. No subsequent studies of the nature of the physical interactions have been reported despite the interest in using CB[*n*] as adsorbents for the removal of CR and related organic dyes from wastewaters. In the present work the supramolecular interaction between CB[*n*] (*n* = 7, 8) and CR was studied by electrospray ionisation mass spectrometry (ESI-MS), ^{1}H NMR, and solid-state characterisation of isolated complexes. Under positive ESI, the formation of host–guest complexes in the gas phase was not observed, suggesting that CR anions do not interact with the portals and the nonpolar inner cavity of the CB[*n*] molecules. Conversely, under negative ESI, 1 : 1 and higher order (1 : 2, 2 : 1, 3 : 1 and 2 : 2) CR : CB[7] and CR : CB[8] adducts were detected, which is attributed to interaction between CR and the outer surface hydrogens of CB[*n*]. Solid-state supramolecular adducts between CB[*n*] and CR were isolated from aqueous media under either ambient conditions, giving structures denoted as CR@CB[*n*](RT), or hydrothermal (100 °C) conditions, giving structures denoted as CR@CB[*n*](100). The adducts were characterised by elemental and thermogravimetric analyses (TGA), powder X-ray diffraction (PXRD), and spectroscopic methods (FT-IR, FT-Raman, ^{13}C{^{1}H} CP MAS NMR, UV/vis and near-IR absorption, fluorescence excitation and emission). The interaction conditions and acid content of the starting CB[*n*] influenced the protonation state of CR molecules. CR@CB[7](RT) contained only unprotonated CR, while CR@CB[8](100) contained exclusively protonated CR (ammonium and azonium/quinoid structures). Other adducts contained mixtures of protonated/unprotonated forms.

Received 14th November 2019,
Accepted 20th January 2020

DOI: 10.1039/c9nj05706d

rsc.li/njc

Introduction

Cucurbiturils (CB[*n*]) are macrocyclic molecules composed of *n* glycoluril units connected by 2*n* methylene bridges.[1–3] The symmetrical geometry of the homologues with *n* = 5–8 creates a nonpolarisable hydrophobic cavity that is accessed *via* two identical, highly electronegative portals made from *n* ureido carbonyls (Fig. 1). CBs are readily prepared from the acid-catalysed condensation reaction of glycoluril and formaldehyde.[4] The homologue CB[6] is the favoured reaction product, especially at higher reaction temperatures (>110 °C). Although the isolation of CB[6] (or possibly a mixture of CB[*n*] homologues) was first described in 1905 by Behrend *et al.*,[5] it was not until the early 1980s that the chemical structure of CB[6] was elucidated by X-ray crystallography.[6] The next major advance occurred in the early 2000s with the optimisation of the synthesis conditions (*e.g.* lower reaction temperatures) to allow the formation of significant amounts of CB homologues (mainly CB[5], CB[7], and CB[8]) in addition to CB[6], which could then be separated in pure form using fractional crystallisation and dissolution techniques.[7,8] Subsequent additions to the CB[*n*] family included CB[10] (as its CB[10]·CB[5] inclusion complex and then, later on, in its free form),[9,10] and CB[13–15], which are distinct from the other homologues since they adopt twisted structures.[11,12]

The supramolecular chemistry of CB[6] was developed in the 1980s and 1990s by Mock,[13] Buschmann,[14] and their co-workers.

[a] *Department of Chemistry, CICECO – Aveiro Institute of Materials, University of Aveiro, Campus Universitário de Santiago, 3810-193 Aveiro, Portugal. E-mail: mpillinger@ua.pt*
[b] *CCMar, and Department of Chemistry and Pharmacy, FCT, University of the Algarve, P-8005-039 Faro, Portugal*
[c] *CQC, Department of Chemistry, University of Coimbra, Rua Larga, 3004-535 Coimbra, Portugal. E-mail: sseixas@ci.uc.pt*

† Electronic supplementary information (ESI) available: General instrumentation details, preparation and/or spectroscopic data for CR and PrCR, full scan and fragmentation ESI-MS spectra, ^{1}H NMR spectra, PXRD patterns, TGA curves, ^{13}C CP MAS NMR spectra and accompanying interpretation. See DOI: 10.1039/c9nj05706d

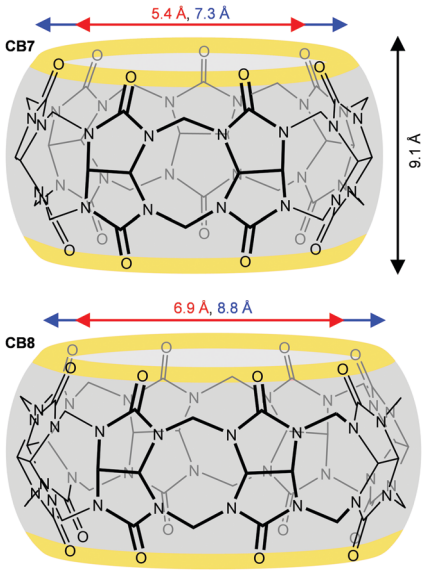

Fig. 1 Structures of CB[*n*] showing the portal (red arrow) and cavity (blue arrow) sizes.

Extensive guest-binding studies showed that the hydrophobic cavity provides an inclusion site for nonpolar molecules, while the carbonyl-lined portals allow CB[6] to bind ions and molecules through charge–dipole and hydrogen-bonding interactions.[15] Hence, CB[6] displays a particular affinity for small organic molecules that combine cationic and hydrophobic subunits in their structure, such as alkylammonium ions. Research on CB supramolecular chemistry increased sharply in the 2000s following the preparation and eventual commercial availability of the homologues CB[5]–CB[8]. The larger cavity sizes of CB[7] and CB[8] enable the encapsulation of more bulky guests such as drug molecules,[16] organometallic compounds,[17,18] and organic dyes.[19,20]

Apart from host–guest chemistry, two other branches of CB chemistry allow the construction of supramolecular assemblies and functional materials. The most familiar of these is the interaction of the CB oxygen atoms with metal ions or clusters.[21–23] The interaction may involve direct coordination or indirect coordination bridged by coordinated water molecules or clusters (*i.e.*, the CB behaves as an outer-sphere ligand). The other branch of CB supramolecular chemistry is founded on weak noncovalent outer-surface interactions, such as C–H$\cdots\pi$ interactions between CH groups of glycoluril segments and aromatic rings, π–π interactions between CB carbonyl groups and aromatic rings, and ion–dipole interactions between the electrostatically positive outer surface of CBs and inorganic or organic anions.[24,25] The resultant supramolecular assemblies have been termed exclusion complexes or lattice inclusion compounds. Aromatic molecules that form such assemblies include 4,4′,4″-benzene-1,3,5-triyl-tribenzoate,[26] 1-anilino-8-naphthalenesulfonate (1,8-ANS),[27,28] 1,5-naphthalenedisulfonate (1,5-NDS),[29] and 2,6-naphthalene-disulfonate.[30]

Looking back to the pioneering work of Behrend *et al.*,[5] it is striking to note that even at this early stage they disclosed the ability of the polymeric substance to form cocrystals (complexes)

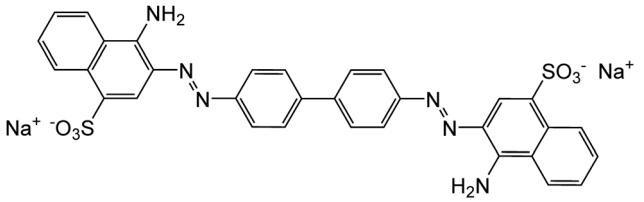

Fig. 2 The chemical structure of the disodium salt of Congo red (CR).

with a variety of substances including $KMnO_4$, $AgNO_3$, H_2PtCl_6, $NaAuCl_4$, Congo red (CR), and methylene blue. For the azo dye CR (Fig. 2), the authors reported that an aqueous solution of the dye was decolourised upon addition of the polymeric substance, with the formation of a red precipitate. CR was the first of many so-called direct dyes and was a huge commercial success for the dye-manufacturing company AGFA.[31,32] Although CR was eventually superseded by superior textile dyes, it has found other uses as a pH indicator[33] and as a histological stain for amyloid.[34] In general, however, most of the contemporary research on CR is conditioned by the fact that CR is toxic to many organisms and metabolises to benzidine, a known human carcinogen.[35,36] Although the marketing to the general public of substances containing CR has been banned in many countries (*e.g.*, since 1999 in the EU), it is still used in some developing countries due to its low cost. Hence, there has been a lot of research on the development of methods for the removal of CR from contaminated wastewater. Adsorption is a proven treatment technology, and a variety of materials have been studied as adsorbents.[37]

Despite the very early revelation by Behrend *et al.* that the glycoluril–formaldehyde condensation product (CB[6]) could decolourise an aqueous solution of CR, no further studies have been reported on the complexation behaviour of cucurbiturils with CR. Such studies may have a wider significance, given the interest in using CB[*n*] as adsorbents for the removal of organic dyes from textile wastewaters.[38–43] Therefore, in the present work, our aim was to achieve a better understanding of complex formation between CR and CB[*n*] (n = 7, 8), using mass spectrometry to detect adduct formation, together with thermal analysis and spectroscopic techniques to characterise the solid complexes that were isolated. The results indicate that in the isolated compounds the CR molecules are trapped within the CB[*n*] lattice, with outer-surface interactions being the likely driving force for the supramolecular assembly.

Experimental

Materials and methods

Setups for general instrumental methods are described in the ESI.† Hydrochloric acid (37% Aldrich) and acetone (p.a., Scharlau) were purchased from commercial sources and used as received. Ultrapure water from a Milli-Q water purifying system was used in all the syntheses. Congo red (CR) [sodium salt of 3,3′-([1,1′-biphenyl]-4,4′-diyl)bis(4-aminonaphthalene-1-sulfonic acid)] was obtained from BDH Chemicals and recrystallised from water : ethanol (1 : 1) before use. Characterisation data (FT-IR band frequencies, ^{1}H NMR and

$^{13}C\{^{1}H\}$ CP MAS NMR chemical shifts) for CR and the protonated blue form of CR (PrCR, prepared as described in the ESI†) are given in the ESI.† The preparation and purification of CB[7] [composition $C_{42}H_{42}N_{28}O_{14}\cdot 11H_2O\cdot 0.1HCl\cdot 0.5(CH_3COCH_3)$] and CB[8] [composition $C_{48}H_{48}N_{32}O_{16}\cdot 7H_2O\cdot 3HCl\cdot 1.5(CH_3COCH_3)$] were described previously.[44,45]

ESI-MS studies

ESI-MS spectra were obtained using a Bruker Daltonics HCT ultra mass spectrometer under positive and negative polarity. Sample solutions were prepared by dissolving CB[*n*] (*n* = 7 or 8) and CR in Milli-Q water to give a final concentration of 50 μM for each component. The samples were analysed immediately after preparation. The ions were continuously generated by infusing the aqueous solutions at 4 μL min^{-1} into the mass spectrometer ion source, with the help of a syringe pump (KdScientific, model 781100, USA). The ion optics and spray parameters were optimised for the signals of CR : CB[*n*] adducts. Typical experimental conditions under negative polarity were as follows: capillary voltage, 3.2 kV; capillary exit voltage, −300 V; skimmer voltage, −15 V; drying gas, 300 °C at 6 L min^{-1}; nebuliser gas pressure, 40 psi. Signal assignments were based on the *m*/*z* values, isotope distributions and fragmentation patterns.

Photophysical characterisation in the solid-state

The absorption spectra of solid samples were recorded on a Cary 5000 UV-vis-NIR spectrophotometer by diffuse reflectance. Before the spectra were obtained, a baseline, with barium sulfate, was collected. The solid-state fluorescence spectra were recorded on a Horiba-Jobin-Ivon SPEX FluoroLog 3-22 spectrofluorimeter using triangular quartz cuvettes. The FluoroLog consists of a modular spectrofluorimeter with double grating excitation (range 200–950 nm, optimised in the UV and with a blazed angle at 330 nm) and emission (range 200–950 nm, optimised in the visible and with a blazed angle at 500 nm) monochromators. The bandpass for excitation and emission was 0–15 nm (values that were continuously adjustable using computer software) and the wavelength accuracy was ±0.5 nm. The excitation source consisted of an ozone-free 450 W Xenon lamp and the emission detector was a Hamamatsu R928 Photomultiplier (200–950 nm range), cooled with a Products for Research thermoelectric refrigerated chamber (model PC177CE005), or a Hamamatsu R5509-42 (900–1400 nm range), cooled to 193 K in a liquid nitrogen chamber (Products for Research model PC176TSCE-005), and a photodiode as the reference detector.[46]

Synthesis of CR:CB supramolecular adducts

Adduct formation between CB[*n*] (*n* = 7 or 8) and CR was performed either at 25 °C in an open system (Schlenk tube) or at 100 °C in a Teflon-lined stainless steel autoclave. The initial CR : CB[*n*] molar ratios were either 1 : 1 (25 °C) or 1.3 : 2 (100 °C).

CR@CB[7](RT). A solution of CR (0.09 g, 0.13 mmol) in water (6 mL) was added to a solution of CB[7] (0.18 g, 0.13 mmol) in water (10 mL) in a Schlenk tube immersed in a temperature-controlled oil bath (25 °C). The mixture was stirred at room temperature for 2 h. The resultant mahogany-coloured solid was separated from the aqueous mother liquor (pH 5–6) by centrifugation, washed with cold water (2 × 5 mL), and finally vacuum-dried. Yield: 0.20 g (68%, based on CB[7]). Anal. calcd for $(C_{42}H_{42}N_{28}O_{14})_{1.15}(C_{32}H_{22}N_6Na_2O_6S_2)\cdot 33H_2O$ (2628.58): C, 36.69; H, 5.23; N, 20.36. Found: C, 36.64; H, 5.02; N, 20.32. TGA revealed a mass loss of 20.0% at 230 °C (calcd for loss of $33H_2O$: 22.6%), and a residual mass of 7.2% at 750 °C (calcd on the basis of a 1 : 0 Na_2CR : PrCR molar ratio: 6.1%).

CR@CB[7](100). A Teflon-lined stainless steel autoclave was charged with CR (0.07 g, 0.10 mmol), CB[7] (0.21 g, 0.15 mmol) and water (10 mL), and heated in an oven at 100 °C for 48 h. The resultant dark red solid was separated from the aqueous mother liquor by filtration, washed with water (5 mL), acetone (5 mL), and finally vacuum-dried. Yield: 0.20 g (72%, based on CB[7]). Anal. calcd for $(C_{42}H_{42}N_{28}O_{14})_{1.6}(C_{32}H_{22.3}N_6Na_{1.7}O_6S_2)\cdot 23H_2O$ (2965.16): C, 40.18; H, 4.61; N, 24.00. Found: C, 39.99; H, 4.44; N, 23.97. TGA revealed a mass loss of 14.4% at 200 °C (calcd for loss of $23H_2O$: 14.0%), and a residual mass of 4.6% at 750 °C (calcd on the basis of a 0.85 : 0.15 Na_2CR : PrCR molar ratio: 4.6%).

CR@CB[8](RT). A solution of CR (0.08 g, 0.12 mmol) in water (6 mL) was added to a suspension of CB[8] (0.20 g, 0.12 mmol) in water (10 mL) in a Schlenk tube immersed in a temperature-controlled oil bath (25 °C). The mixture was stirred at room temperature for 24 h. The resultant dark purple solid was separated from the aqueous mother liquor (pH 3) by centrifugation, washed with cold water (6 mL), and finally vacuum-dried. Yield: 0.27 g (94%, based on CB[8]). Anal. calcd for $(C_{48}H_{48}N_{32}O_{16})_{1.05}(C_{32}H_{23.3}N_6Na_{0.7}O_6S_2)\cdot 22H_2O$ (2459.98): C, 40.23; H, 4.82; N, 22.55. Found: C, 40.04; H, 4.37; N, 22.51. TGA revealed a mass loss of 16.6% at 200 °C (calcd for loss of $22H_2O$: 16.1%), and a residual mass of 2.2% at 750 °C (calcd on the basis of a 0.35 : 0.65 Na_2CR : PrCR molar ratio: 2.3%).

CR@CB[8](100). A Teflon-lined stainless steel autoclave was charged with CR (0.07 g, 0.10 mmol), CB[8] (0.25 g, 0.15 mmol) and water (10 mL), and heated in an oven at 100 °C for 48 h. The resultant reddish-purple solid was separated from the aqueous mother liquor by filtration, washed with water (10 mL), and finally vacuum-dried. Yield: 0.20 g (62%, based on CB[8]). Anal. calcd for $(C_{48}H_{48}N_{32}O_{16})_{1.3}(C_{32}H_{24}N_6O_6S_2)\cdot 19H_2O$ (2722.82): C, 41.64; H, 4.61; N, 24.49. Found: C, 41.63; H, 4.43; N, 24.41. TGA revealed a mass loss of 10.4% at 230 °C (calcd for loss of $19H_2O$: 12.5%), and a residual mass of 0% at 750 °C.

Results and discussion

ESI-MS and ^{1}H NMR studies

The supramolecular interaction between cucurbiturils and CR was first evaluated by ESI-MS. ESI-MS has been used to study the formation of cucurbituril host–guest complexes[47] and their aggregates[48] as well as the interaction between negative ions and the outer surface hydrogens of these molecular containers.[49] Initially, the formation of complexes between CR and both macrocycles under positive polarity was evaluated. CR and CB[*n*] were

dissolved in water (50 μM CR, 50 μM CB[*n*]) and the solutions analysed immediately. The main signals observed were assigned to free hosts and aggregates of free hosts (Fig. S1, ESI†). The absence of signals corresponding to host–guest complexes under positive ESI suggests that CR is not interacting with the inner cavity of the studied cucurbiturils.

To obtain further insights into the interaction between CR and CB[*n*], the formation CR@CB[7] complexes was studied by ^{1}H NMR. CB[7] gave the expected ^{1}H NMR signals, while CR, as reported,[50] showed weak and broad signals (Fig. S2, ESI†). After addition of CR to CB[7] at 1 : 1 stoichiometry (1 mM) CR signals were not detected and CB[7] peaks broadened (Fig. S2, ESI†). No signals assignable to CR–CB[7] interaction were detected by ^{1}H NMR. Unlike that observed for CR@cyclodextrins,[50] CB[7] does not sharpen CR signals. In fact, a precipitate was observed inside the NMR tube, which explains the absence of CR peaks and indicates that CB[7] is interacting with CR leading to its precipitation. Similar behaviour was observed for 1,8-ANS and CB[*n*] (*n* = 6, 7).[27,28] For CB[7], a 2 : 1 complex with 1,8-ANS sandwiched between the outer surface of two CB[7] was proposed.[28] Liu *et al.* described a similar type of supramolecular framework with 1,5-NDS anions interacting with CB[6] through hydrogen bonding.[51]

To evaluate the possible interaction between CR anions and the outer surface hydrogens of CB[*n*] the formation of complexes/aggregates under negative ESI was studied. Interaction between CB[*n*] and anions has been observed under negative ESI and associated with interactions with the outer surface hydrogens of CB[*n*].[49] CR : CB[7] and CR : CB[8] adducts are readily observed in the gas phase after analysis of aqueous solutions containing 50 μM CR and 50 μM CB[*n*] (Fig. 3 and Fig. S3 in the ESI†). Signal assignments were based on the *m*/*z* values, isotope distributions and fragmentation patterns (see, for example, Fig. 4, which shows the fragmentation spectrum for *m*/*z* 1243.2). Besides 1 : 1 (CR : CB[*n*]) adducts, higher order 1 : 2, 2 : 1, 3 : 1 and 2 : 2 aggregates were observed. The presence in the solutions of aggregates with even higher order cannot be excluded. They might have *m*/*z* values higher than the upper limit of the instrument used or, most likely, be destroyed during the electrospray. The formation of CR–CB[*n*] aggregates must be due to interaction between CR anions and the outer surface hydrogens of CB[*n*].

Isolation and characterisation of CR@CB[*n*] adducts

To isolate CR@CB[*n*] adducts, a solution of CR in water was added to either a solution (CB[7]) or a solution/suspension (CB[8]) of the cucurbituril in water, with the CR : CB[*n*] molar ratio being set at 1 : 1, and the reaction mixtures were stirred at room temperature (RT) for either 2 h (for CB[7]) or 24 h (for CB[8]). The resultant suspensions were centrifuged to isolate a mahogany-coloured solid in the case of CR@CB[7](RT) and a dark purple solid in the case of CR@CB[8](RT). PXRD analysis indicated that both solids had amorphous character, with only three very broad peaks being present in the 2θ range of 5–30° (Fig. S4, ESI†). In an effort to improve the crystallinity of the compounds, a second set of reactions was performed in which a 50% excess of CB[*n*] was used (CR : CB[*n*] = 1.3 : 2) and the mixtures were subjected to a hydrothermal treatment at 100 °C for 48 h in a Teflon-lined stainless steel autoclave. The PXRD pattern of the dark red CB[7] solid product, denoted CR@CB[7](100), was unchanged from that for CR@CB[7](RT), while the pattern for the reddish-purple CB[8] solid product, CR@CB[8](100), displayed several fairly narrow reflections in the 2θ range of 5–30° characteristic of a microcrystalline structure (Fig. S4, ESI†). These reflections do not match with those of the as-prepared CB[8] sample nor with those present in previously reported experimental or computed diffractograms for CB[8] hydrate phases,[45] indicating that the CB molecules in CR@CB[8](100) adopt a different crystal packing arrangement. None of the PXRD patterns for the CR@CB[*n*] adducts display peaks assignable to a pure (bulk) CR phase, suggesting that the isolated solids are not physical mixtures of CB[*n*] and CR phases.

Elemental analyses (CHN) indicated final CB[*n*]/CR molar ratios of 1.15 for CR@CB[7](RT), 1.05 for CR@CB[8](RT), 1.6 for CR@CB[7](100), and 1.3 for CR@CB[8](100). Water contents were estimated from the TGA weight losses between room temperature and 200–230 °C (Fig. S5, ESI†). Apart from the different initial weight losses due to the variable water contents, the TGA curves for CR@CB[7](100) and CR@CB[8](100) almost overlapped, with the onset of decomposition being at about 300 °C. Decomposition took place in two consecutive

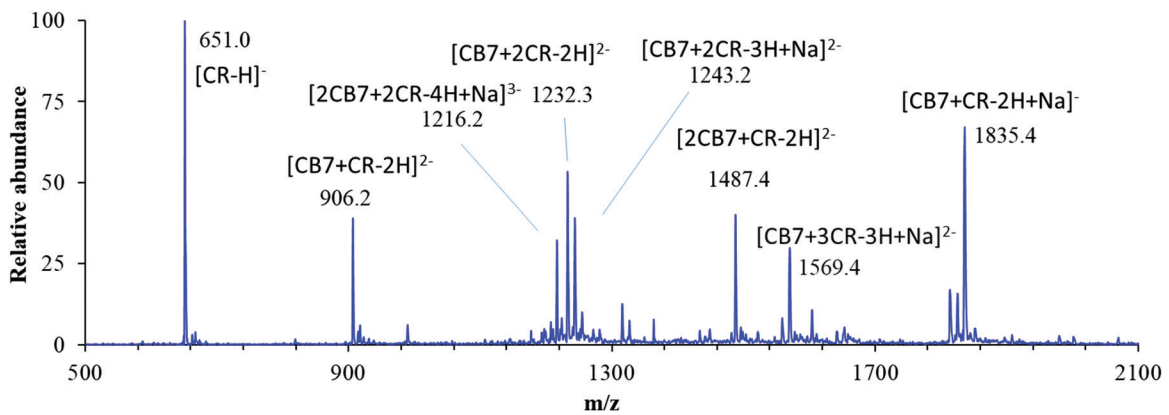

Fig. 3 Full scan spectrum of aqueous solutions of CR@CB[7] (50 μM : 50 μM) under negative ESI. The *m*/*z* values are of the first peak of the isotope series.

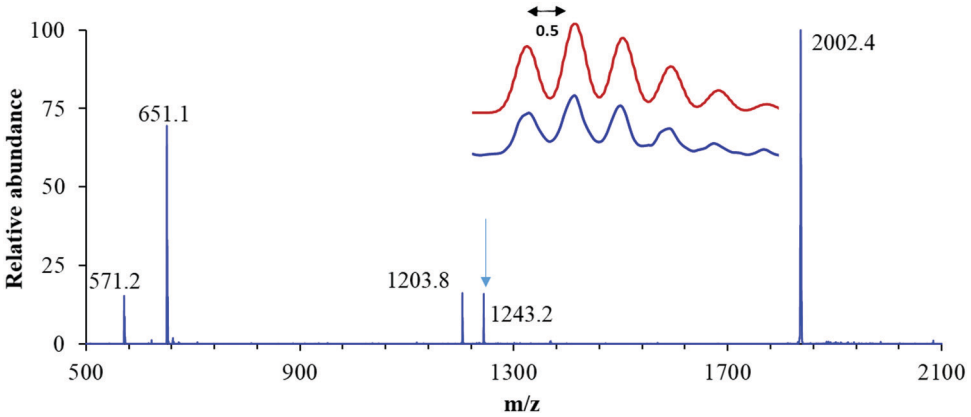

Fig. 4 Fragmentation spectrum (MS^2) of *m/z* 1243.2. The arrow indicates the fragmented peak. The inset shows the experimental (blue) and simulated (red) isotope distributions.

steps identified by DTG_{max} (DTG = derivative thermogravimetric) values of 400 and 500 °C. The CB[*n*] molecules in these two adducts seem to possess slightly higher thermal stability than the pure as-prepared CB[7] and CB[8] samples, which displayed DTG_{max} values of 380 ± 5 °C. Pure CR decomposes in two steps up to 535 °C with the abrupt mass losses giving DTG_{max} values of 315 and 492 °C (Fig. S5, ESI†). Based on the elemental compositions proposed for the isolated CR@CB[*n*] solids and the observation of a 12.9% mass loss for the first step in the TGA curve of pure CR, a mass loss step of 3.0–3.6% would be expected to be present at *ca.* 315 °C in the TGA curves of CR@CB[*n*] if the solids were physical mixtures rather than true supramolecular adducts. No such step was visible in any of the curves. As found for CR@CB[*n*](100), the TGA curves for CR@CB[*n*](RT) are very similar. However, despite the fact that these compounds start to decompose at a similar temperature to that for CR@CB[*n*](100) (*ca.* 300 °C), decomposition of the organic components in CR@CB[*n*](RT) takes place over a wider temperature range (up to 700 °C), with a final step being observed with DTG_{max} = 615 ± 5 °C.

The residual masses registered at 750 °C by TGA are different for each of the CR@CB[*n*] adducts, decreasing in the order CR@CB[7](RT) (7.2%) > CR@CB[7](100) (4.6%) > CR@CB[8](RT) (2.2%) > CR@CB[8](100) (0%). The residue obtained from the thermal decomposition of pure CR (23% mass at 750 °C) is composed mainly of Na_2SO_4.[52] As will be discussed below, the different residual Na_2SO_4 masses recorded in the TGA curves of the CR@CB[*n*] adducts can be attributed to the presence of the anionic (*i.e.*, disodium salt) and/or protonated (sodium-free) forms of CR in different proportions.

The FT-IR spectra of the adducts CR@CB[*n*](RT/100) are dominated by bands due to the CB molecules (Fig. 5). In general, these bands are unshifted relative to those for as-prepared CB[7] and CB[8]. With reference to the spectrum of CR (Fig. 5(a)), the spectra for the adducts present two bands that can be assigned to the azo dye, namely a band at 1043 cm^{-1} due to the symmetric stretching vibration of the sulfonate group, and a broad absorption centred at 1612 cm^{-1} assigned to an aromatic ring C–C stretching vibration. The relative intensities of these two bands

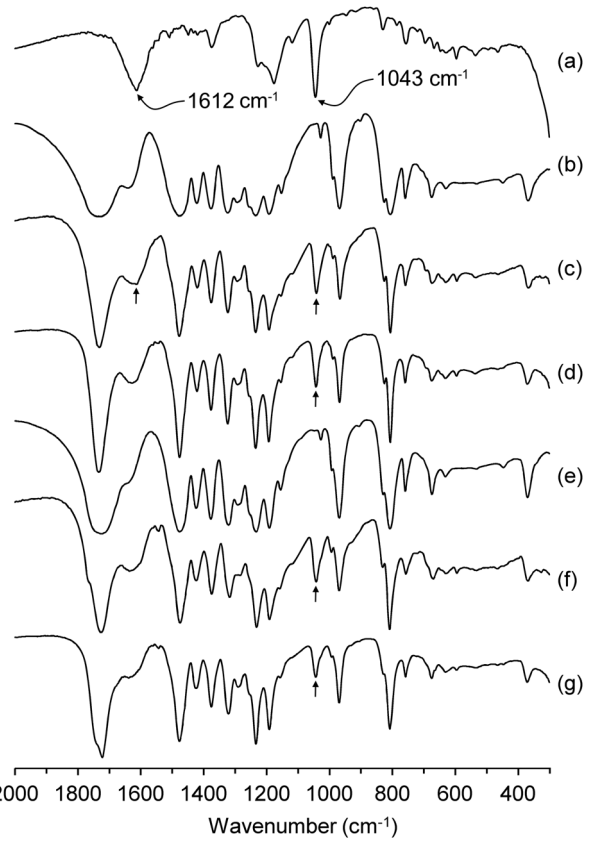

Fig. 5 FT-IR spectra in the range of 300–2000 cm^{-1} for (a) CR, (b) CB[7], (c) CR@CB[7](RT), (d) CR@CB[7](100), (e) CB[8], (f) CR@CB[8](RT), and (g) CR@CB[8](100). CR bands at 1043 and 1612 cm^{-1} are indicated with arrows.

decrease on going from CR@CB[*n*](RT) to CR@CB[*n*](100), which is consistent with the elemental analyses that indicate lower CR contents for the latter.

Fig. 6 shows the FT-Raman spectra of the CR@CB[*n*] adducts in the range of 1000–1800 cm^{-1}. In contrast to the IR spectra, the Raman spectra are dominated by bands due to CR. The spectrum for CR@CB[7](RT) (Fig. 6(d)) is essentially identical to

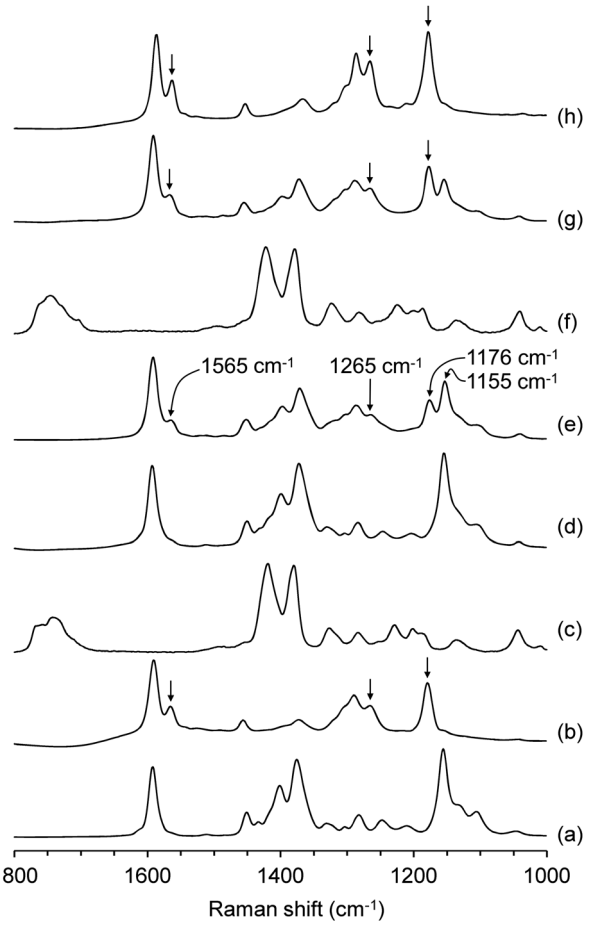

Fig. 6 FT-Raman spectra in the range of 1000–1800 cm^{-1} for (a) CR, (b) PrCR, (c) CB[7], (d) CR@CB[7](RT), (e) CR@CB[7](100), (f) CB[8], (g) CR@CB[8](RT), and (h) CR@CB[8](100). The bands at 1176, 1265 and 1565 cm^{-1} in spectrum (e) are attributed to PrCR; corresponding bands in spectra (b, g and h) are indicated with arrows.

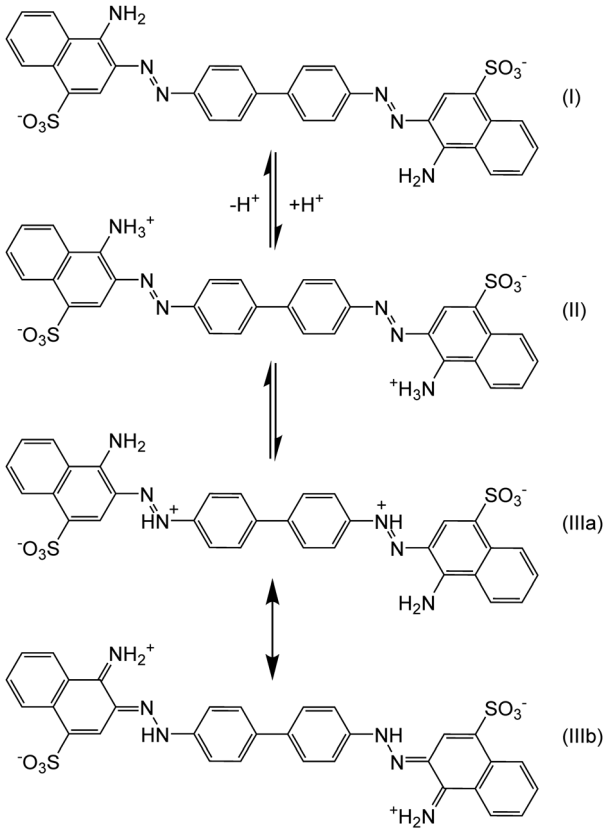

Scheme 1 Protonation mechanism for CR in acidic solution:[33,52] Anionic form (I), ammonium tautomer (II), azonium tautomer (IIIa) and its resonant quinoid structure (IIIb).

that for CR (Fig. 6(a)). On the other hand, additional bands at 1176, 1265 and 1565 cm^{-1} are present for CR@CB[7](100) (Fig. 6(e)), which are attributed to a protonated form of CR. The band at 1176 cm^{-1} appears alongside a more intense band at 1155 cm^{-1}. The latter is assigned to a phenyl-N= stretching mode of an azoic structure (*i.e.*, unprotonated anionic CR and/or protonated ammonium form), while the new high-frequency band is assigned to a N–N stretching vibration of a quinoid structure (Scheme 1).[33] This assignment was confirmed by isolating the protonated form of CR (PrCR), which precipitates as a blue solid upon addition of dilute HCl to an aqueous solution of CR (pH < 2.7). The Raman spectrum of PrCR (Fig. 6(b)) displays bands at 1179, 1265 and 1565 cm^{-1}, which are in accordance with the new bands observed for CR@CB[7](100).

The protonation mechanism of CR has been well studied due to its use as an acid–base indicator and as a histological stain for amyloid proteins.[33,34] Protonation of CR in water occurs below a pH of 5.3 and has been proposed to give an ammonium form (II) and a resonance-stabilised azonium form (III), which are in tautomeric equilibrium (Scheme 1).[33,53] The colour transition from red to blue has been associated with the formation of resonant quinoid structures. In the synthesis of CR@CB[7](RT), the mother liquor had a final pH of 5–6 and therefore the exclusive presence of the anionic form (I) in the isolated adduct is not surprising. Performing the synthesis under hydrothermal conditions (100 °C) with a 50% excess of CB[7] gave an adduct containing a mixture of the unprotonated and protonated (ammonium and/or azonium) forms of CR, with the former probably being the major form present. Since the as-prepared CB[8] sample had a much higher HCl content (*ca.* 3 equivalents) than CB[7], the synthesis of CR@CB[8](RT) led to a mother liquor with a pH of 2–3, and the Raman spectrum of the isolated adduct indicates that a higher proportion of quinoid structures is present (Fig. 6(g)). The Raman spectrum of the sample prepared under hydrothermal conditions, CR@CB[8](100), is consistent with an even higher proportion of quinoid structures (Fig. 6(h)). The prevalence of the protonated or unprotonated forms of CR in the CR@CB[*n*] adducts was indicated by the colours of the isolated solids since the CB[7] compounds were dark red while the CB[8] compounds were purple.

The trends observed in the Raman spectra regarding the relative proportions of the azoic and resonance-stabilised azonium forms of CR are consistent with the different residual Na_2SO_4 masses registered in the TGA curves of the adducts. The lack of any residue for CR@CB[8](100) (0 mass% at 750 °C)

indicates that the as-synthesised adduct only contained a protonated form of CR (*i.e.*, containing no sodium ions). On the basis of the 23 mass% value obtained at 750 °C in the TGA curve of pure CR, the relative proportions of the unprotonated anionic and protonated ammonium and/or azonium forms of CR can be estimated for the different adducts: 1 : 0 for CR@CB[7](RT), 0.85 : 0.15 for CR@CB[7](100), 0.35 : 0.65 for CR@CB[8](RT), and 0 : 1 for CR@CB[8](100). This trend aligns well with the different relative intensities displayed by each adduct for the Raman vibrational bands assigned to the azoic/azonium forms of CR.

$^{13}C\{^{1}H\}$ CP MAS NMR spectra for the CR@CB[*n*] adducts were consistent with other measurements in indicating that on going from CR@CB[*n*](RT) to CR@CB[*n*](100) the CR content decreases as does the relative proportion of the unprotonated form of CR. The spectra are presented and discussed in the ESI.†

Photophysical data for CR@CB[*n*] adducts

Electronic spectra were obtained for the samples CR@CB[7](100) and CR@CB[8](100). The reader is referred to ref. 54 for a detailed analysis of the absorption, fluorescence, and fluorescence excitation spectra of CR in solution (water or dimethylsulfoxide) and in the solid-state (as the disodium salt or intercalated in a layered double hydroxide host).

The UV-vis (200–1000 nm) and near-IR (NIR; 1000–2500 nm) absorption spectra of the solid samples CR@CB[*n*](100) are shown in Fig. 7, and compared with those for CR, PrCR and CB[*n*] in the solid-state, and CR in aqueous solution. In the UV-vis range, where electronic transitions for the two free cucurbiturils are absent (with the exception of shoulders at ~250 nm for CB[8] and ~280 nm for CB[7]), three bands are observed in the spectra of the adducts with maxima at 349, 505 and 725 nm for CR@CB[7](100), and at 349, 527 and 750 nm for CR@CB[8](100). The broad band system between 600 and 800 nm is absent for CR in water at neutral pH. Pigorsch *et al.* measured absorption spectra of aqueous CR solutions as a function of pH.[33] At neutral pH, the solution is orange-red, and the principal absorption band has a maximum at 497 nm and is assigned to a π–π* transition of the azo group. As the pH is lowered to 5.3, the solution turns violet, the 497 nm band shifts slightly to 520 nm, and new overlapping broad bands appear with maxima at 665 and 730 nm.[33,54] Pigorsch *et al.* assigned the absorption band at 520 nm to the ammonium form (II in Scheme 1), which preserves the azoic structure (and thus the band is not shifted far from the corresponding band for unprotonated CR at neutral pH), while the band system between 600 and 800 nm was assigned to the protonated azonium form of CR (III in Scheme 1), where the formation of a quinoid structure causes an absorption at longer wavelengths. We may therefore attribute the absorption maxima at 527 and 750 nm for CR@CB[8](100) to the protonated ammonium and azonium forms, respectively. This assignment is in accordance with the similarity of the absorption spectra for CR@CB[8](100) and PrCR in the solid-state (Fig. 7A). For CR@CB[7](100), the broad band system between 600 and 800 nm is relatively less intense than that for the CB[8] adduct, and the absorption maximum for the band associated with the azoic structure appears at the shorter wavelength of 505 nm. The latter broad band probably comprises overlapping bands due to the unprotonated anionic form of CR (~497 nm) and the protonated ammonium form (~527 nm). Hence, the absorption spectra for the CR@CB[*n*] adducts are consistent with the other characterisation data discussed above, showing that CR@CB[7](100) contains a mixture of the unprotonated anionic and protonated (ammonium/azonium) forms of CR, while CR@CB[8](100) only contains the latter.

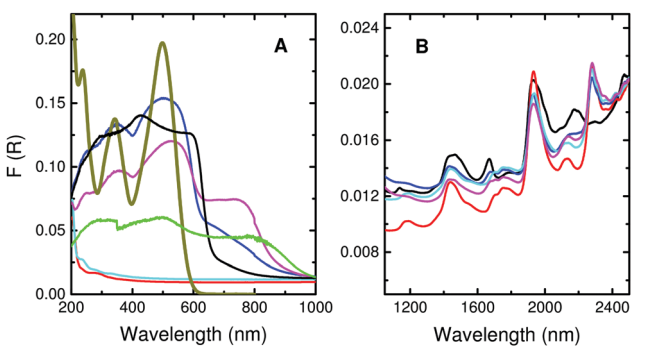

Fig. 7 Diffuse reflectance absorbance spectra (Kubelka–Munk scale) in the UV-vis (A) and NIR (B) ranges for CR (black), PrCR (green), CB[7] (red), CR@CB[7](100) (blue), CB[8] (cyan), and CR@CB[8](100) (magenta). The absorption spectrum of CR in water (dark yellow) is shown for comparison.

In the NIR range (Fig. 7B), the spectra for CB[7] and CB[8] are practically identical, showing bands assigned[55] to the second overtone of the methylene C–H stretching vibration (1182 nm, 8460 cm^{-1}), a combination band involving the symmetric and asymmetric stretching modes of water molecules (1432 nm, 6983 cm^{-1}), the first overtone of the methylene C–H stretching vibration (1745 nm, 5731 cm^{-1}), and a combination band of O–H stretching and HOH bending modes (1935 nm, 5168 cm^{-1}). The assignment of two other bands at longer wavelengths is less clear; the band at 2125 nm (4706 cm^{-1}) may be due to a combination of C–H and C=O stretching modes, while the stronger band at 2280 nm (4386 cm^{-1}) may be due to a combination of C–H stretching and CH_2 deformation modes. These six bands for the CB[*n*] molecules are present in the spectra of the CR@CB[*n*](100) adducts and are essentially unshifted. In fact, the spectra of the pure CB[*n*] molecules and the respective adducts are very similar, although careful comparison of these spectra with that for CR in the solid-state reveals the presence of some additional bands for the adducts that can be assigned to the organic dye molecule. In the region 1300–1750 nm, pure CR displays two bands with absorption maxima at ~1465 nm (6826 cm^{-1}) and 1667 nm (6000 cm^{-1}), which are tentatively assigned to the first overtones of N–H and aromatic C–H stretching vibrations, respectively. The former band is just visible as a weak shoulder in the spectra of the adducts, while the latter band is more prominent, especially for the adduct CR@CB[7](100).

The fluorescence emission data for CR@CB[7](100) show that while the supramolecular interaction of CR with CB[7] does not lead to improved emission properties, it does lead to a

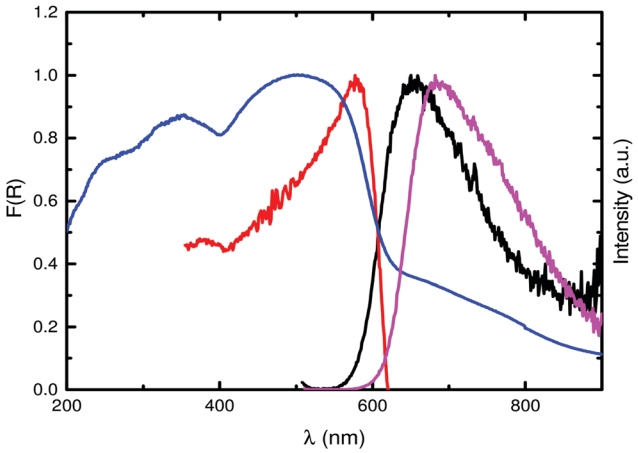

Fig. 8 Absorption (blue), fluorescence excitation (red, λ_{em} = 650 nm) and emission spectra (black, λ_{exc} = 490 nm) of CR@CB[7](100). The emission spectrum of CR in the solid state is shown for comparison (magenta, λ_{exc} = 490 nm).

blue-shift of the emission band from 680 nm for CR itself to around 655 nm for the adduct (Fig. 8).

Conclusions

The mechanism by which cucurbiturils decolourise an aqueous solution of the azo dye Congo red is of interest, especially from the perspective of using CB[*n*] to remove CR and related dyes from wastewater. In the present work, we have shown that ESI-MS is an effective technique to investigate CR–CB[*n*] interactions in the gas phase and can distinguish between the formation of host–guest inclusion complexes and outer-surface adducts. The data show that CR forms the latter type of complex with CB[7] and CB[8]. The major operative interactions are likely to be π–π interactions of the carbonyl groups of CB[*n*] with the aromatic rings of CR, and CH···O hydrogen bonds involving the sulfonate oxygen atoms and CH or CH_2 groups on the periphery of CB[*n*] molecules. The combined effect of these interactions is sufficiently strong to result in the removal of CR from aqueous solution through the formation of insoluble exclusion compounds, also known as lattice inclusion compounds. Depending on the type of CB[*n*] homologue and the reaction conditions (pH, temperature), different forms of CR can be immobilised, from the unprotonated dianion to the protonated neutral molecule as the ammonium and/or azonium tautomers, the latter of which is stabilised through resonance with a quinoid structure.

Conflicts of interest

There are no conflicts to declare.

Acknowledgements

This study had the support of national funds provided by the FCT (Portuguese Foundation for Science and Technology) and MCTES (Portuguese Ministry of Science, Technology and Higher Education) through the strategic projects CICECO – Aveiro Institute of Materials (UID/CTM/50011/2019), CCMAR (UID/Multi/04326/2019) and the Coimbra Chemistry Centre (UID/QUI/00313/2019). We are grateful for funding provided through the operational programmes CRESC Algarve 2020 and COMPETE 2020 (project EMBRC.PT ALG-01-0145-FEDER-022121), and CENTRO 2020 (project CENTRO-01-0145-FEDER-028031, PTDC/QUI-QOR/28031/2017), co-financed by national funds through the FCT/MEC and the European Union through the European Regional Development Fund under the Portugal 2020 Partnership Agreement.

Notes and references

1 J. Lagona, P. Mukhopadhyay, S. Chakrabarti and L. Isaacs, The Cucurbit[*n*]uril Family, *Angew. Chem., Int. Ed.*, 2005, **44**, 4844–4870.
2 E. Masson, X. Ling, R. Joseph, L. Kyeremeh-Mensah and X. Lu, Cucurbituril chemistry: a tale of supramolecular success, *RSC Adv.*, 2012, **2**, 1213–1247.
3 K. I. Assaf and W. M. Nau, Cucurbiturils: from synthesis to high-affinity binding and catalysis, *Chem. Soc. Rev.*, 2015, **44**, 394–418.
4 H. Cong, X. L. Ni, X. Xiao, Y. Huang, Q.-J. Zhu, S.-F. Xue, Z. Tao, L. F. Lindoy and G. Wei, Synthesis and separation of cucurbit[*n*]urils and their derivatives, *Org. Biomol. Chem.*, 2016, **14**, 4335–4364.
5 R. Behrend, E. Meyer and F. Rusche, I. Ueber Condensationsproducte aus Glycoluril und Formaldehyd, *Justus Liebigs Ann. Chem.*, 1905, **339**, 1–37.
6 W. A. Freeman, W. L. Mock and N.-Y. Shih, Cucurbituril, *J. Am. Chem. Soc.*, 1981, **103**, 7367–7368.
7 J. Kim, I.-S. Jung, S.-Y. Kim, E. Lee, J.-K. Kang, S. Sakamoto, K. Yamaguchi and K. Kim, New Cucurbituril Homologues: Syntheses, Isolation, Characterization, and X-ray Crystal Structures of Cucurbit[*n*]uril (*n* = 5, 7, and 8), *J. Am. Chem. Soc.*, 2000, **122**, 540–541.
8 A. Day, A. P. Arnold, R. J. Blanch and B. Snushall, Controlling Factors in the Synthesis of Cucurbituril and Its Homologues, *J. Org. Chem.*, 2001, **66**, 8094–8100.
9 A. I. Day, R. J. Blanch, A. P. Arnold, S. Lorenzo, G. R. Lewis and I. Dance, A Cucurbituril-Based Gyroscane: A New Supramolecular Form, *Angew. Chem., Int. Ed.*, 2002, **41**, 275–277.
10 S. Liu, P. Y. Zavalij and L. Isaacs, Cucurbit[10]uril, *J. Am. Chem. Soc.*, 2005, **127**, 16798–16799.
11 X.-J. Cheng, L.-L. Liang, K. Chen, N.-N. Ji, X. Xiao, J.-X. Zhang, Y.-Q. Zhang, S.-F. Xue, Q.-J. Zhu, X.-L. Ni and Z. Tao, Twisted Cucurbit[14]uril, *Angew. Chem., Int. Ed.*, 2013, **52**, 7252–7255.
12 Q. Li, S.-C. Qiu, J. Zhang, K. Chen, Y. Huang, X. Xiao, Y. Zhang, F. Li, Y.-Q. Zhang, S.-F. Xue, Q.-J. Zhu, Z. Tao, L. F. Lindoy and G. Wei, Twisted Cucurbit[n]urils, *Org. Lett.*, 2016, **18**, 4020–4023.

13 W. L. Mock, *Cucurbituril*, in *Supramolecular Chemistry II - Host Design and Molecular Recognition*, ed. E. Weber, Top. Curr. Chem., Springer, Berlin, Heidelberg, 1995, vol. 175, pp. 1–24.
14 R. Hoffmann, W. Knoche, C. Fenn and H.-J. Buschmann, Host–guest complexes of cucurbituril with the 4-methylbenzylammonium ion, alkali-metal cations and NH_4^+, *J. Chem. Soc., Faraday Trans.*, 1994, **90**, 1507–1511.
15 S. J. Barrow, S. Kasera, M. J. Rowland, J. del Barrio and O. A. Scherman, Cucurbituril-Based Molecular Recognition, *Chem. Rev.*, 2015, **115**, 12320–12406.
16 D. Das, K. I. Assaf and W. M. Nau, Applications of Cucurbiturils in Medicinal Chemistry and Chemical Biology, *Front. Chem.*, 2019, **7**, 619.
17 D. P. Buck, P. M. Abeysinghe, C. Cullinane, A. I. Day, J. G. Collins and M. M. Harding, Inclusion complexes of the antitumour metallocenes Cp_2MCl_2 (M = Mo, Ti) with cucurbit[*n*]urils, *Dalton Trans.*, 2008, 2328–2334.
18 C. I. R. Magalhães, A. C. Gomes, A. D. Lopes, I. S. Gonçalves, M. Pillinger, E. Jin, I. Kim, Y. H. Ko, K. Kim, I. Nowik and R. H. Herber, Ferrocene and ferrocenium inclusion compounds with cucurbiturils: a study of metal atom dynamics probed by Mössbauer spectroscopy, *Phys. Chem. Chem. Phys.*, 2017, **19**, 21548–21555.
19 R. N. Dsouza, U. Pischel and W. M. Nau, Fluorescent Dyes and Their Supramolecular Host/Guest Complexes with Macrocycles in Aqueous Solution, *Chem. Rev.*, 2011, **111**, 7941–7980.
20 A. C. Bhasikuttan, H. Pal and J. Mohanty, Cucurbit[*n*]uril based supramolecular assemblies: tunable physicochemical properties and their prospects, *Chem. Commun.*, 2011, **47**, 9959–9971.
21 O. A. Gerasko, M. N. Sokolov and V. P. Fedin, Mono- and polynuclear aqua complexes and cucurbit[6]uril: Versatile building blocks for supramolecular chemistry, *Pure Appl. Chem.*, 2004, **76**, 1633–1646.
22 X.-L. Ni, X. Xiao, H. Cong, L.-L. Liang, K. Cheng, X.-J. Cheng, N.-N. Ji, Q.-J. Zhu, S.-F. Xue and Z. Tao, Cucurbit[*n*]uril-based coordination chemistry: from simple coordination complexes to novel poly-dimensional coordination polymers, *Chem. Soc. Rev.*, 2013, **42**, 9480–9508.
23 J. Lü, J.-X. Lin, M.-N. Cao and R. Cao, Cucurbituril: A promising organic building block for the design of coordination compounds and beyond, *Coord. Chem. Rev.*, 2013, **257**, 1334–1356.
24 X.-L. Ni, X. Xiao, H. Cong, Q.-J. Zhu, S.-F. Xue and Z. Tao, Self-Assemblies Based on the "Outer-Surface Interactions" of Cucurbit[*n*]urils: New Opportunities for Supramolecular Architectures and Materials, *Acc. Chem. Res.*, 2014, **47**, 1386–1395.
25 M. Zhang, R.-L. Lin, W.-Q. Sun and J.-X. Liu, Anion encapsulation and complexation by cucurbit[n]urils and their derivatives, *J. Inclusion Phenom. Macrocyclic Chem.*, 2018, **90**, 173–187.
26 K. Chen, Y.-S. Kang, Y. Zhao, J.-M. Yang, Y. Lu and W.-Y. Sun, Cucurbit[6]uril-Based Supramolecular Assemblies: Possible Application in Radioactive Cesium Cation Capture, *J. Am. Chem. Soc.*, 2014, **136**, 16744–16747.
27 B. D. Wagner and A. I. MacRae, The Lattice Inclusion Compound of 1,8-ANS and Cucurbituril: A Unique Fluorescent Solid, *J. Phys. Chem. B*, 1999, **103**, 10114–10119.
28 B. D. Wagner, N. Stojanovic, A. I. Day and R. J. Blanch, Host Properties of Cucurbit[7]uril: Fluorescence Enhancement of Anilinonaphthalene Sulfonates, *J. Phys. Chem. B*, 2003, **107**, 10741–10746.
29 L. Liu, Z. Zhao and C. Hao, 3D fluorescent cucurbit[7]uril framework linked by anion fluorophore, *J. Inclusion Phenom. Macrocyclic Chem.*, 2017, **88**, 247–252.
30 X. Gao, Z. Xu, M. Liu and P. Zhang, A novel CB[6]-based supramolecular assembly exhibiting highly selective multi-responsive fluorescence sensing for trace amounts of Fe^{3+} ions and acetone molecules, *J. Solid State Chem.*, 2019, **271**, 110–114.
31 D. P. Steensma, "Congo" Red. Out of Africa?, *Arch. Pathol. Lab. Med.*, 2001, **125**, 250–252.
32 C. J. Cooksey, Quirks of dye nomenclature. 2. Congo red, *Biotech. Histochem.*, 2014, **89**, 384–387.
33 E. Pigorsch, A. Elhaddaoui and S. Turrell, Spectroscopic study of pH and solvent effects on the structure of Congo red and its binding mechanism to amyloid-like proteins, *Spectrochim. Acta, Part A*, 1994, 2145–2152.
34 E. I. Yakupova, L. G. Bobyleva, I. M. Vikhlyantsev and A. G. Bobylev, Congo Red and amyloids: history and relationship, *Biosci. Rep.*, 2019, **39**, BSR20181415.
35 M. Hernández-Zamora, F. Martínez-Jerónimo, E. Cristiani-Urbina and R. O. Cañizares-Villanueva, Congo red dye affects survival and reproduction in the cladoceran *Ceriodaphnia dubia*. Effects of direct and dietary exposure, *Ecotoxicology*, 2016, **25**, 1832–1840.
36 M. Hernández-Zamora and F. Martínez-Jerónimo, Congo red dye diversely affects organisms of different trophic levels: a comparative study with microalgae, cladocerans, and zebrafish embryos, *Environ. Sci. Pollut. Res.*, 2019, **26**, 11743–11755.
37 N. P. Raval, P. U. Shah and N. K. Shah, Adsorptive amputation of hazardous azo dye Congo red from wastewater: a critical review, *Environ. Sci. Pollut. Res.*, 2016, **23**, 14810–14853.
38 S. Karcher, A. Kornmüller and M. Jekel, Removal of Reactive Dyes by Sorption/Complexation with Cucurbituril, *Water Sci. Technol.*, 1999, **40**, 425–433.
39 H. J. Nagy, P. Sallay, M. L. Varga, I. Rusznák, P. Bakó and A. Víg, Removal of Dyes from Industrial Wastewater by Cucurbiturils, *Text. Res. J.*, 2009, **79**, 1312–1318.
40 X. Xie, X. Li, H. Luo, H. Lu, F. Chen and W. Li, The Adsorption of Reactive Blue 19 Dye onto Cucurbit[8]uril and Cucurbit[6]uril: An Experimental and Theoretical Study, *J. Phys. Chem. B*, 2016, **120**, 4131–4142.
41 X. Li, X. Xie, H. Luo, L. Li, Z. Li, Z. Xue and W. Li, Adsorption of reactive yellow X-RG and reactive brilliant red X-3B onto cucurbit[8]uril and cucurbit[6]uril: Effect factors, adsorption behavior and mechanism study, *J. Colloid Interface Sci.*, 2017, **498**, 31–46.

42 H. Luo, X. Huang, Y. Luo, Z. Li, L. Li, C. Gao, J. Xiong and W. Li, Adsorption behavior and mechanism of acidic blue 25 dye onto cucurbit[8]uril: A spectral and DFT study, *Spectrochim. Acta, Part A*, 2018, **193**, 125–132.

43 P. Zhang, X. Gao, M. Liu, L. Liang, H. Li and Y. Wang, The effective adsorption of Reactive Blue 19 Dye with a cucurbit[6]uril based supramolecular assembly, *Inorg. Chem. Commun.*, 2018, **96**, 13–15.

44 S. M. Bruno, A. C. Gomes, T. S. M. Oliveira, M. M. Antunes, A. D. Lopes, A. A. Valente, I. S. Gonçalves and M. Pillinger, Catalytic alcoholysis of epoxides using metal-free cucurbituril-based solids, *Org. Biomol. Chem.*, 2016, **14**, 3873–3877.

45 A. C. Gomes, C. I. R. Magalhães, T. S. M. Oliveira, A. D. Lopes, I. S. Gonçalves and M. Pillinger, Solid-state study of the structure and host–guest chemistry of cucurbituril-ferrocene inclusion complexes, *Dalton Trans.*, 2016, **45**, 17042–17052.

46 J. Seixas de Melo, T. Costa, A. Francisco, A. L. Maçanita, S. Gago and I. S. Gonçalves, Dynamics of short as compared with long poly(acrylic acid) chains hydrophobically modified with pyrene, as followed by fluorescence techniques, *Phys. Chem. Chem. Phys.*, 2007, **9**, 1370–1385.

47 M. Pessêgo, J. Mendoza, J. P. Da Silva, N. Basílio and L. Garcia-Rio, Unveiling the Formation 1:2 Supramolecular Complexes Between Cucurbit[7]uril and a Cationic Calix[4]arene Derivative, *Chem. Commun.*, 2019, **55**, 13828–13831.

48 J. P. Da Silva, N. Jayaraj, S. Jockusch, N. J. Turro and V. Ramamurthy, Aggregates of Cucurbituril Complexes in the Gas Phase, *Org. Lett.*, 2011, **13**, 2410–2413.

49 M. A. A. Rodrigues, D. C. Mendes, V. Ramamurthy and J. P. Da Silva, ESI-MS of Cucurbituril Complexes Under Negative Polarity, *J. Am. Soc. Mass Spectrom.*, 2017, **28**, 2508–2514.

50 S. Kobayashi, S. Miwa, I. Tanaka, K. Mikuni, M. Miura, S. Ogawa and K. Takahashi, Dospectral Analyses of Interaction between Congo Red and Cyclodextrins at Various pH, *J. Appl. Glycosci.*, 2008, **55**, 173–177.

51 L. Liu, Y. Yao, X. Zhang and C. Hao, A Fluorescent 1,5-Naphthalenedisulfonate Anion-Linked Cucurbit[6]uril Framework, *Eur. J. Org. Chem.*, 2015, 6806–6810.

52 Z. Yermiyahu, A. Landau, A. Zaban, I. Lapides and S. Yariv, Monoionic montmorillonites treated with Congo red, *J. Therm. Anal. Calorim.*, 2003, **72**, 431–441.

53 Z. Yermiyahu, I. Lapides and S. Yariv, Thermo-visible-absorption spectroscopy study of the protonated Congo-red montmorillonite complex, *Appl. Clay Sci.*, 2007, **37**, 1–11.

54 A. L. Costa, A. C. Gomes, M. Pillinger, I. S. Gonçalves, J. Pina and J. S. Seixas de Melo, Insights into the photophysics and supramolecular organization of Congo red in solution and the solid state, *ChemPhysChem*, 2017, **18**, 564–575.

55 J. Workman Jr and L. Weyer, *Practical Guide to Interpretive Near-Infrared Spectroscopy*, CRC Press, Taylor & Francis Group, Boca Raton, 2008.

